



Computational and in vitro analyses on synergistic effects of paclitaxel and thymoquinone in suppressing invasive breast cancer cells

Mohammad Rsool Khazaei¹ · Maryam Bozorgi¹ · Mozafar Khazaei¹ · Alireza Moradi² · Azam Bozorgi^{1,3}

Received: 3 January 2024 / Accepted: 7 February 2024
© The Author(s), under exclusive licence to Springer Nature B.V. 2024

Abstract

Background In the present experiment, we evaluated the impact of thymoquinone (TQ) and paclitaxel (PTX) treatment on MDA-MB-231 cell line growth inhibition via controlling apoptosis/autophagy.

Materials and results MDA-MB-231 cells were exposed to PTX (0, 25, 50, 75, and 100 nM), TQ (0, 25, 50, 75, and 100 μ M), and combinations for 48 h. After the MTT assessment, dose-response curves and IC₅₀ values were calculated, and the combination synergism was evaluated using the Compusyn software. Following the treatment with PTX, TQ, and combinations at IC₅₀ doses, the expression of apoptosis and autophagy genes was assessed in cells. The GraphPad Prism program was used to analyze the data, and Tukey's test at $p < 0.05$ was then run. PTX, TQ, and their combinations inhibited MDA-MB-231 cell proliferation and viability dose-dependently. TQ reduced the effective concentration (IC₅₀) of PTX in co-treatment groups. PTX and TQ showed antagonistic effects when cell proliferation declined above 70%. Antagonistic effects shifted into additive and synergistic effects upon increasing PTX concentration, indicated by diminished cell proliferation below 70%. PTX-TQ co-treatment significantly enhanced P53 and BAX expression while reducing Bcl-2 expression. Also, their combination increased Beclin-1, ATG-5, and ATG-7 expression in treated cells.

Conclusion Effective concentrations of TQ and PTX had synergic effects and inhibited breast cancer cells via prompting apoptosis and autophagy in vitro.

Keywords Breast neoplasm · Paclitaxel · Thymoquinone · Apoptosis · Autophagy

Introduction

Breast cancer (BC) is the most frequent malignancy diagnosed among females and both sex populations, which replaced lung cancer in 2020 with an anticipated 2.3 million global cases and approximately 685,000 deaths [1]. Close to 25% of all the globe-diagnosed BC cases were observed in Eastern Asia; 50% of all deaths were reported

in the East, Southeast, and South Center regions of Asia [2]. BC is a genetically multifaceted disease with complex heterogeneity classified into distinct molecular subtypes expressing either estrogen receptor (ER+), progesterone receptor (PR+), and human epidermal growth factor receptor 2 (HER2+). Subtypes lacking the hormone receptor expression are triple-negative BC (TNBC) [3]. Screening disease at early stages, high-resolution imaging technology, and highly effective chemo-, radio-, and immunotherapies have improved patients' quality of life and life expectancy [3, 4]. However, metastatic BC, including TNBC that dynamically undergoes genetic variations and biological heterogeneity, remains incurable, with tumor recurrence in one-third of patients who received chemotherapy within three years post-diagnosis [3]. Paclitaxel (PTX) is an FDA-approved chemotherapy drug from the taxane family, widely used as a first-line treatment in different kinds of cancers, including advanced metastatic BC, ovarian and hormone-refractory prostate malignancies, and non-small cell lung cancer [5]. PTX interferes with microtubule dynamics by

✉ Azam Bozorgi
abozorgi1991@gmail.com

¹ Fertility and Infertility Research Center, Health Technology Institute, Kermanshah University of Medical Sciences, Kermanshah, Iran

² Student Research Committee, Kermanshah University of Medical Sciences, Kermanshah, Iran

³ Department of Tissue Engineering, School of Medicine, Kermanshah University of Medical Sciences, Kermanshah, Iran

binding and stabilizing them in the polymerized form during cell division. PTX-stabilized microtubules fail to segregate chromosomes during mitosis, leading to cell cycle arrest and apoptosis induction [5, 6]. Due to poor water solubility, the clinically administered PTX contains additive compounds raising side effects like hypersensitivity, nephrotoxicity, neurotoxicity, and hypersensitive reactions [7]. In addition, PTX resistance observed in BC patients is generally attributed to β -tubulin gene mutation, the over-expression of tubulin-associated protein Tau, ER, HER2, BRCA1, and P-glycoprotein [8]. It has been suggested that combining chemotherapeutic agents with phytochemicals enhances tumor sensitization, reduces tumor drug resistance and recurrence, and declines organ toxicities and unfavorable outcomes following chemotherapy [9]. A well-known phytochemical with various pharmacological and biological benefits is thymoquinone (TQ). TQ is a biologically active component derived from black seeds (*Nigella sativa*) with potent anti-inflammatory, antioxidant, analgesic, anticancer, hepato-, and neuroprotective properties [10]. TQ inhibits BC cell proliferation, motility, and invasion by targeting signaling pathways like NF- κ B and PI3K/ Akt and stimulating cell cycle arrest and apoptosis [11]. Clinical trials in advanced and metastatic BC patients approved that the co-administration of curcumin with PTX was safe and efficacious in improving the objective response rate and physical function over 12 weeks post-treatment [12]. However, most studies indicate the beneficial synergistic of drug combinations, but the precise combination effect is not well investigated. In the present experiment, we explored binary combinations of PTX with TQ and their impact on inhibiting MDA-MB-231 cells through regulating apoptosis/autophagy.

Materials and methods

Materials thymoquinone (TQ, Cat# 274,666), paclitaxel (PTX, Cat# T7191), and dimethyl sulfoxide (DMSO, Cat# D8418) were purchased from Sigma (Sigma-Aldrich Chemie GmbH, Taufkirchen, Germany). DMEM-F12 medium (Cat# 10,565,018), fetal bovine serum (FBS, Cat# 16-000-044), and MTT reagent (Cat# M6494) were obtained from Gibco (Gibco Invitrogen, Massachusetts, USA).

Cell line provision and culture

The MDA-MB-231 cell line (human breast adenocarcinoma, NCBI Code: C578) was purchased (Pasteur Institute of Iran, Tehran, Iran) and grew in the DMEM-F12 media supplemented with 10% FBS, and 1% antibiotics (100 U/ml penicillin and 100 μ g/ml streptomycin). Cells were

incubated at 37 °C and 5% CO₂ in a humidified incubator, and the culture medium was replaced twice weekly til cells reached 80% confluent.

Drug treatment and experimental group design

MDA-MB-231 cells were detached from culture flasks using the trypsin/EDTA solution, centrifuged, and resuspended in DMEM-F12 medium containing 10% FBS, and 1% antibiotics. Suspended cells were cultivated in 96-well plates at 10⁴ cells/well density and left in the incubator for 24 h. Cells were then exposed to a range of PTX (25, 50, 75, 100 nM), TQ (25, 50, 75, 100 μ M), and four combination groups (a constant concentration of TQ (25, 50, 75, 100 μ M) + different concentrations of PTX (25, 50, 75, 100 nM)) for 48 h. Cells treated neither with PTX nor TQ were considered as the control sample.

Cell proliferation and IC50 calculation

The MTT (3-(4,5-dimethylthiazol-2-yl)-2,5-diphenyltetrazolium bromide) test method was used to examine cell proliferation after drug treatment. Accordingly, after the cell treatment, the culture medium from plate wells was replaced with 200 μ L MTT solution (0.5 mg/mL) per well, and the plate was incubated at 37 °C for 3 h. Then, the MTT reagent was pulled out, and formazan crystals were dissolved by adding 200 μ L of dimethyl sulfoxide (DMSO). The optical density (OD) for samples was read using the ELISA reader instrument (Biorad, Hercules, CA, USA) at 570 nm. Accordingly, cell proliferation was computed as follows:

$$\text{Cell proliferation (\%)} = \frac{OD_T}{OD_C} \times 100$$

In the equation, OD_T is the OD for cells that received treatments, and OD_C is the OD for untreated cells.

IC50 value, described as a concentration in which 50% of cell proliferation is inhibited, was computed for each group by plotting the dose-response curves in GraphPad Prism software.

Cell viability

The impact of drug treatments on cell viability was measured using the LDH (lactate dehydrogenase) test. As mentioned, MDA-MB-231 cells were exposed to PTX, TQ, and their combinations for 48 h. A group of untreated cells were regarded for measuring Total LDH content. LDH contents were measured using the LDH assay kit (Kiazist, Iran) and followed the manufacturer's recommendation. Total LDH was analyzed by adding 20 μ L Permisolution to each well

in the Total LDH group and then leaving the plate at 25 °C for an hour. For analyzing the LDH content, 50 µL of supernatants from each well were aspirated and transferred to a 96-well plate, followed by adding 50 µL working buffer and incubating the plate at 37 °C for 30 min. The sample OD was read in the ELISA reader instrument at 545 nm and the cell viability was calculated accordingly:

$$\text{Cellviability} = 1 - \left(\frac{\text{OD}_{\text{Test}} - \text{OD}_{\text{Control}}}{\text{OD}_{\text{Total}} - \text{OD}_{\text{Control}}} \times 100 \right)$$

OD_{Test} is the OD of cells that received treatments, OD_{Control} is the OD of cells that received no treatments, and OD_{Total} is the OD of the Total LDH group.

Analysis of drug combination

PTX and TQ interactions and their impact on cell proliferation were evaluated using the Compusyn software version 1.0 (Biosoft, Ferguson, MO, USA) by calculating quantitative data of combination index (CI), dose reduction index (DRI), and isobologram graph according to Chou description [13]. The median effect analysis was used to determine the CI values, classified as CI < 1 for synergism, CI = 1 for additive effects, and CI > 1 for antagonism.

Apoptosis and autophagy measurement

A quantitative Real-time polymerase chain reaction (PCR) method was utilized for assessing the expression of apoptosis (P53, BAX, Bcl-2) and autophagy (Beclin-1, ATG-5, ATG-7) genes. MDA-MB-231 cells were exposed to IC50 doses of PTX, TQ, and their combinations for 48 h under standard culture conditions. Cells without treatments were regarded as the control group. After treatments, cells were collected by detaching using EDTA/trypsin and centrifuging; then, the

Total RNA extraction was carried out using the Trizol agent (Life Biolab, Heidelberg, Germany), followed by measuring RNA concentrations using the NanoDrop 2000 Spectrophotometer (Thermo Scientific, Germany, Deutschland). 1 µg of RNA samples and the RevertAid First Strand cDNA Synthesis Kit (ThermoFisher Scientific Inc., Porto Salvo, Portugal) were applied for synthesizing cDNA, according to the manufacturer's instructions. Real-time PCR was performed using the cDNA, high-ROX SYBR green PCR Master Mix (RealQ Plus 2x Master Mix, Ampliqon, Denmark), and specific forward and reverse primers listed in Table 1, in the Step One Real-time PCR machine (Applied Biosystems, USA). The quantitative values of the comparative threshold cycle (CT) were obtained for each sample and normalized against the glyceraldehyde 3-phosphate dehydrogenase (GAPDH) as the internal control. Relative gene expression data were computed using the 2^{-(ΔΔCT)} formula and reported as the fold change.

Statistic evaluation

Three triplicates (*n*=3) of the quantitative data were obtained and presented as Mean ± SD. GraphPad Prism program (Version 7, GraphPad Software, San Diego, CA, USA) was used to analyze the data using one-way analysis of variance (ANOVA) and a Tukey's test at the significant level of P-value < 0.05.

Results

Cell proliferation and IC50 calculation

The MTT data of MDA-MB-231 cells exposed to PTX, TQ, and their combinations is shown in Fig. 1. PTX and TQ reduced cell proliferation dose-dependently (***) P-value <

Table 1 The list of Forward and Reverse primers

Gene	Accession no.	Sequence (5'→3')	Length (bp)	Annealing temperature (°c)
Human P53	NM_001126118.2	F: 5'- TAACAGTTCTGCATGGGCGGC -3'	21	60
		R: 5'- AGGACAGGCACAAACACGCACC -3'	22	
Human BAX	NM_001291430.2	F: 5'- CCTGTGCACCAAGGTGCCGGAAC -3'	24	60
		R: 5'- CCACCCTGGTCTTGGATCCAGCCC -3'	24	
Human Bcl-2	NM_000657.3	F: 5'- TTGTGGCCTTCTTGAGTTCGGTG -3'	24	60
		R: 5'- GGTGCCGGTTCAGGTAAGTCA -3'	24	
Human Beclin1	XM_017025264.3	F: 5'- CTGGACACTCAGCTCAACGTCA -3'	22	60
		R: 5'- CTCTAGTGCCAGCTCCTTAGC-3'	22	
Human ATG5	XM_054356851.1	F: 5'- GCAGATGGACAGTTGCACACAC -3'	22	60
		R: 5'- GAGGTGTTTCCAACATTGGCTCA -3'	22	
Human ATG7	XM_054344959.1	F: 5'- CGTTGCCACAGCATCATCTTC -3'	22	60
		R: 5'- CACTGAGGTTCAACATCCTTGG -3'	22	
Human GAPDH	NM_001289745.3	F: 5'-AAGGTCGGAGTCAACGGATTG-3'	22	60
		R: 5'-GCCATGGGTGGAATCAATTGG-3'	22	

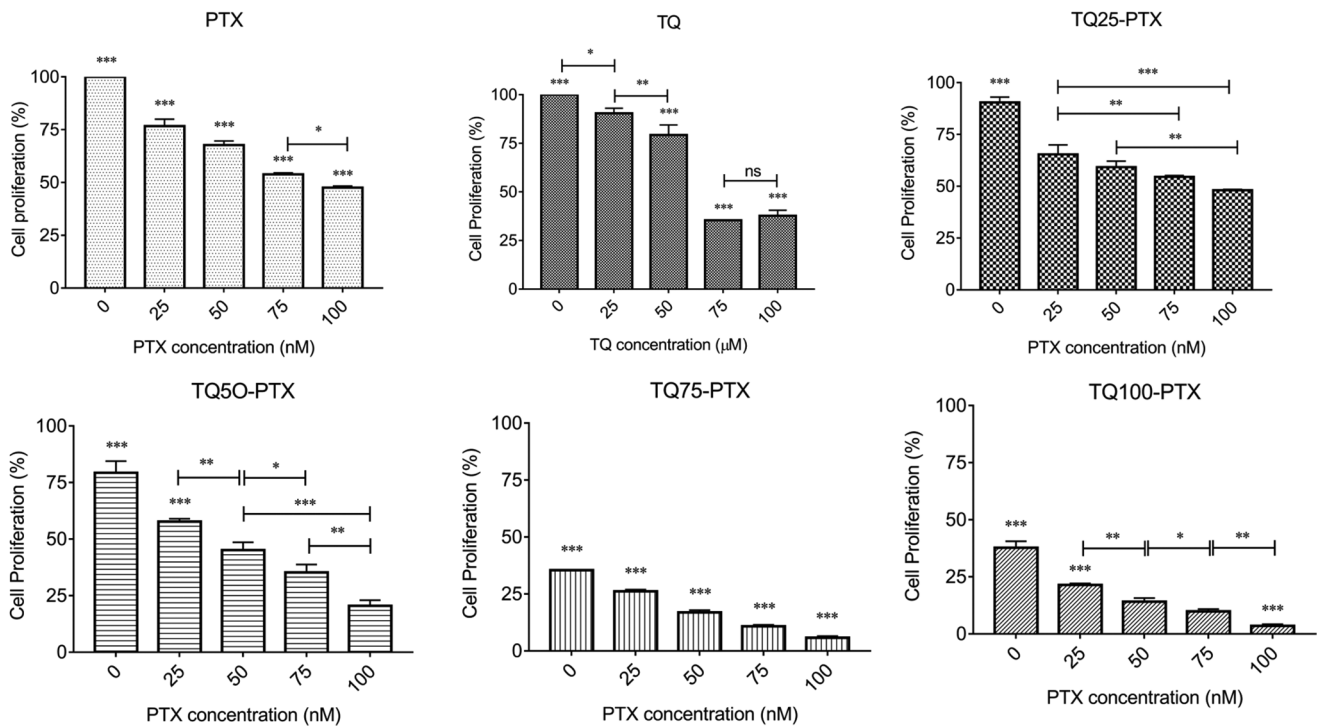


Fig. 1 The MTT data of MDA-MB-231 cells treated with PTX, TQ, and their combinations for 48 h. PTX and TQ reduced cell proliferation dose-dependently. Co-treatment with TQ and PTX decreased cell

proliferation correlated with PTX concentration (***) P-value < 0.001, ** P-value < 0.01, * P-value < 0.05, ns: non-significant)

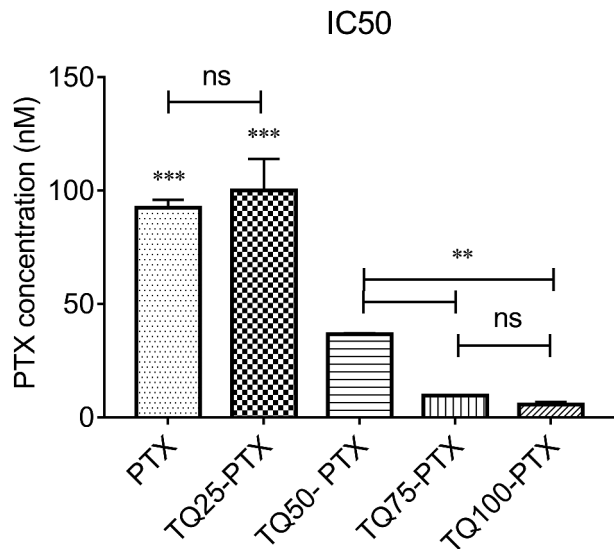


Fig. 2 IC₅₀ values of PTX alone and in combination with TQ25 μM, TQ50 μM, TQ75 μM, and TQ100 μM, respectively. IC₅₀ values of PTX lowered when combined with TQ, especially at 50, 75, and 100 μM concentrations (***) P-value < 0.001, ** P-value < 0.01, ns: non-significant)

0.001, ** P-value < 0.01, * P-value < 0.05). Also, co-treatment with TQ and PTX resulted in a remarkable reduction in cell proliferation, which was correlated with PTX concentration at constant TQ doses (***) P-value < 0.001, ** P-value < 0.01, * P-value < 0.05, ns: non-significant).

IC₅₀ values obtained from dose-response curves are shown in Fig. 2. Accordingly, IC₅₀ values were 77 ± 2.9 μM for TQ (data are not shown), and 92.45 ± 3.5 nM, 100.2 ± 13.9 nM, 36.7 ± 0.4 nM, 9.6 ± 0.2 nM, and 5.75 ± 1.1 nM for PTX at single (uncombined) state, and combination with TQ25 μM, TQ50 μM, TQ75 μM, and TQ100 μM respectively. These data indicated that IC₅₀ values of PTX were reduced when combined with TQ at 50, 75, and 100 μM concentrations (***) P-value < 0.001, ** P-value < 0.01, ns: non-significant).

Cell viability

The viability results for MDA-MB-231 cells exposed to PTX, TQ, and their combinations are shown in Fig. 3. Cell viability decreased in groups treated with PTX and TQ dose-dependent (***) P-value < 0.001, ** P-value < 0.01). Meanwhile, cell viability prominently declined in co-treatment groups compared to single-treated groups. At co-treatment groups with constant TQ concentration, cell viability

diminished with increasing PTX dose (***) P-value < 0.001, ** P-value < 0.01, * P-value < 0.05).

Drug combination analysis

Interactions between PTX and TQ in co-treatments were computationally analyzed to evaluate if synergistic effects were observed. Combination index (CI), isobologram, and dose-reduction index (DRI) graphs are depicted in Fig. 4 (a, b, c) and Fig. 5 (a, b). As seen in Fig. 4a, the antagonism effect was observed when the proliferation (Fa) of MDA-MB-231 cells co-treated with PTX and TQ declined but was above 70% (CI > 1). At the same time, the synergistic effect resulted in cell proliferation dropping below 70%. The detailed evaluation of CI in treatment groups (Fig. 4b) revealed that co-treatment with low doses of PTX (25 and 50 nM) appeared as antagonism (CI > 1) and additive effects (CI = 1). Upon co-treatment with high amounts of PTX (75 and 100 nM), antagonism effects became attenuated and shifted towards synergistic outcomes (CI < 1). The isobologram graph (Fig. 4c) also confirmed the synergistic effect of co-treatments at IC50 values.

After determining PTX-TQ interaction effects, DRI values were computed for effective doses (ED) at 95%, 75%, 50%, and 25% cell proliferation (Fig. 5a, b). DRI refers to how many folds of dose reduction are permitted in a synergistic combination at a designated response level compared

to single drugs. DRI > 1 suggests the positive interaction between drugs, giving rise to reducing effective doses [14]. As seen in Fig. 5b, DRI values at ED25, ED50, ED75, and ED95 are 5.31, 2.97, 1.66, and 0.63 for PTX and 2.38, 2.52, 2.67, and 2.93 for TQ. These data pointed out that PTX significantly reduced the effective dose of TQ at all cell proliferation states (Fa). At the same time, TQ had the same effect on PTX at 75%, 50%, and 25% cell proliferation (***) P-value < 0.001, ** P-value < 0.01, * P-value < 0.05).

Apoptosis and autophagy measurement

After MDA-MB-231 cells were treated with IC50 concentrations of PTX, TQ, and their combination for 48 h, the expression of apoptotic (P53, BAX, Bcl-2) and autophagic (Beclin-1, ATG-5, ATG-7) genes were evaluated (Figs. 6 and 7). The P53 level was prominently higher in treated groups than in untreated (control) cells. P53 values were 2.25, 2.16, 3.15, 3.27, 4.1, and 4.7 in PTX, TQ, PTX+TQ 25 μ M, PTX+TQ 50 μ M, PTX+TQ 75 μ M, and PTX+TQ 100 μ M groups. Statistically different P53 expression was observed between the control, PTX+TQ 75 μ M and PTX+TQ 100 μ M with all experimental groups (***) P-value < 0.001, ns: non-significant). BAX expression increased in treatment samples with remarkably differences in all groups (***) P-value < 0.001). BAX values expanded to 5.76, 3.9, 8.02, 10.14, 10.54, and 11.35 folds in PTX, TQ,

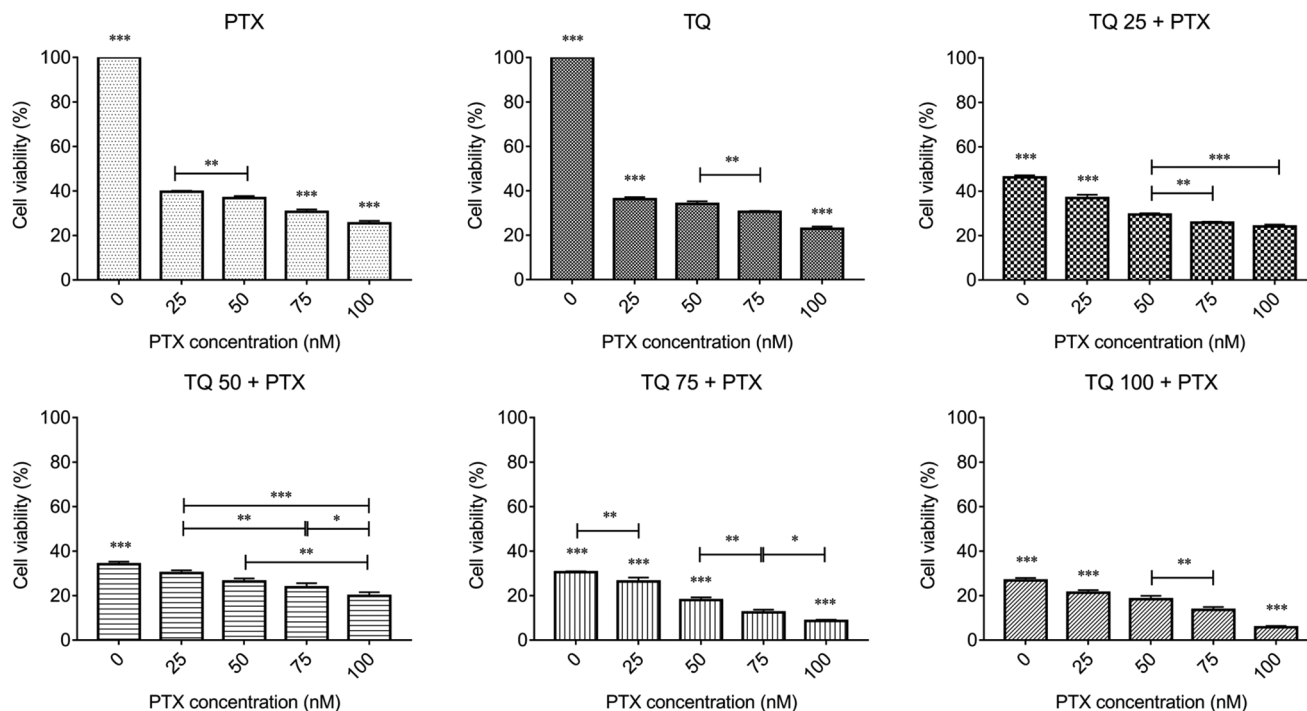


Fig. 3 The LDH data of MDA-MB-231 cells treated with PTX, TQ, and their combinations for 48 h. PTX and TQ reduced cell survival dose-dependently. Co-treatment with TQ and PTX decreased cell viability

correlated with PTX concentration (***) P-value < 0.001, ** P-value < 0.01, * P-value < 0.05)

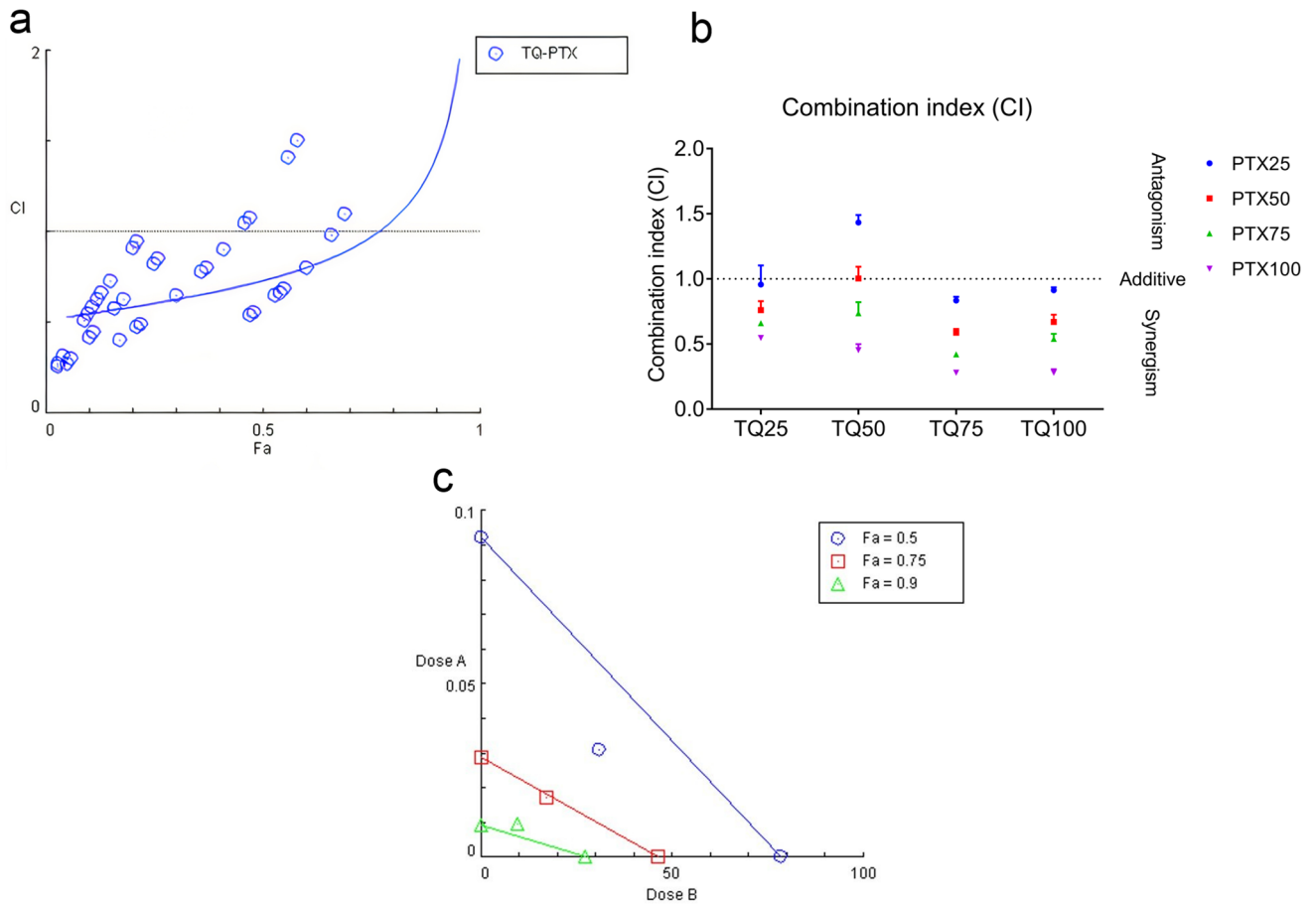


Fig. 4 The computational analysis of PTX and TQ interactions in MDA-MB-231 cells co-treated with PTX, TQ, and their combinations for 48 h; **a**: combination index (CI) graph for TQ-PTX at various cell responses to treatment (cell proliferation) (Fa); **b**: CI values for co-treatment groups; **c**: isobologram for TQ-PTX at cell proliferation 50%, 75%, and 90%

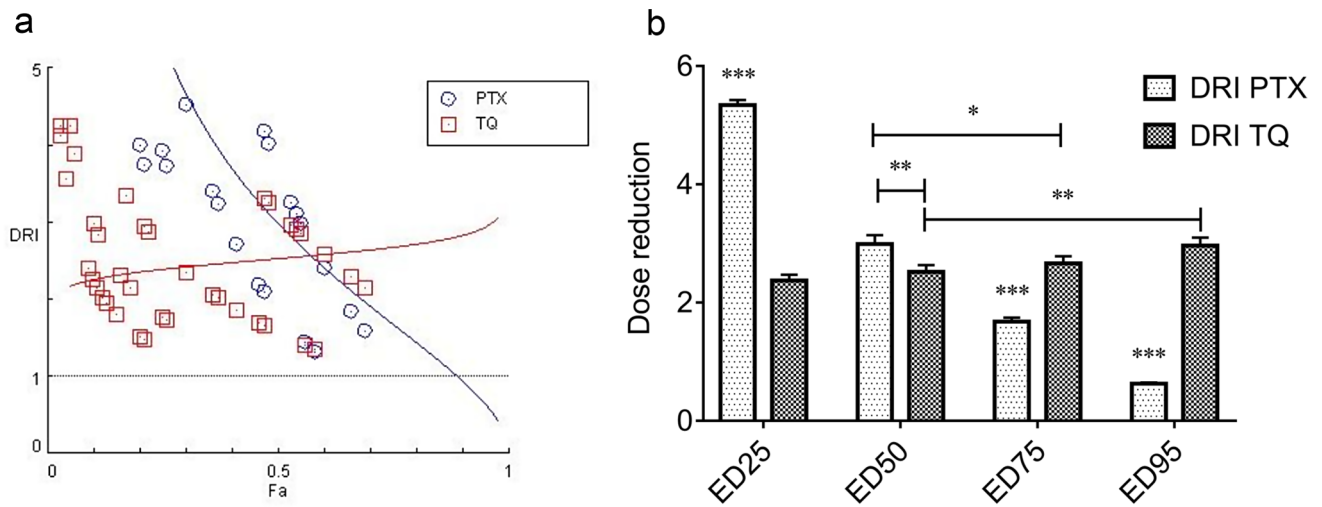


Fig. 5 Dose-reduction index (DRI) for PTX and TQ co-treatments; **a**: DRI values at different cell responses to treatment (cell proliferation) (Fa); **b**: DRI values for effective doses (ED) at 95%, 75%, 50%, and 25% cell proliferation (***) P-value < 0.001, ** P-value < 0.01, * P-value < 0.05)

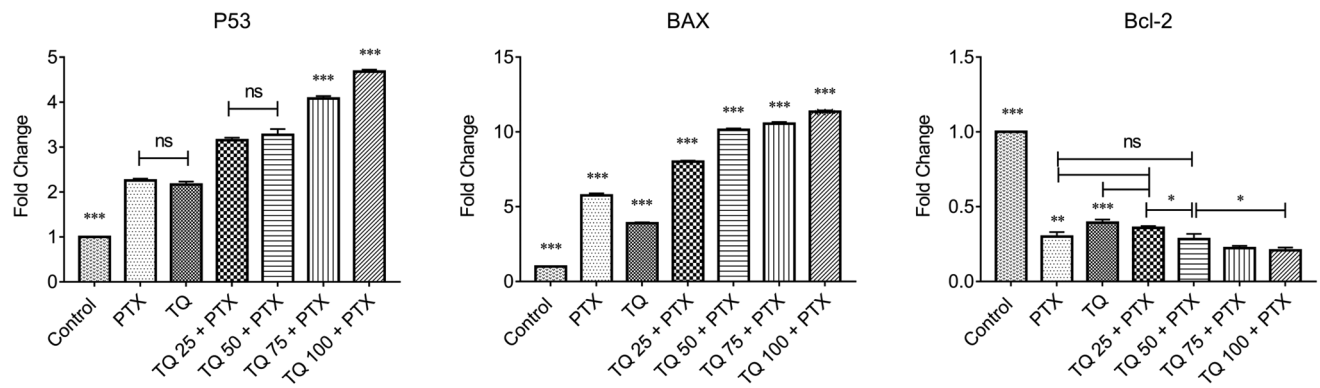


Fig. 6 The expression of P53, BAX, and Bcl-2 apoptotic genes in MDA-MB-231 cells co-treated with IC50 concentrations of PTX, TQ, and their combinations for 48 h. The combination of TQ and PTX increased the expression of pro-apoptotic P53 and BAX while decreasing the expression of anti-apoptotic Bcl-2 (***) P-value < 0.001, ** P-value < 0.01, * P-value < 0.05, ns: non-significant)

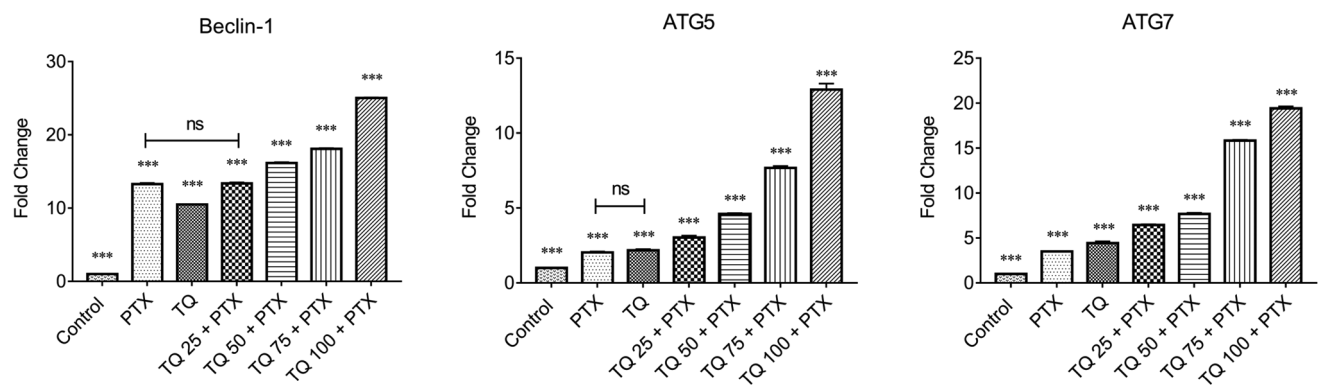


Fig. 7 The expression of Beclin-1, ATG-5, and ATG-7 autophagic genes in MDA-MB-231 cells co-treated with IC50 concentrations of PTX, TQ, and their combinations for 48 h. The combination of TQ and PTX increased the expression of autophagic genes (***) P-value, ns: non-significant)

PTX + TQ 25 μ M, PTX + TQ 50 μ M, PTX + TQ 75 μ M, and PTX + TQ 100 μ M groups. Bcl-2 expression diminished significantly in treatment groups compared with the control sample. Bcl-2 values were 0.3, 0.4, 0.36, 0.28, 0.22, and 0.21 folds in PTX, TQ, PTX + TQ 25 μ M, PTX + TQ 50 μ M, PTX + TQ 75 μ M, and PTX + TQ 100 μ M groups (***) P-value < 0.001, ** P-value < 0.01, * P-value < 0.05, ns: non-significant).

Beclin-1 expression grew significantly in treated cells than the control ones, and remarkable differences were evident between nearly most treatment groups. Beclin-1 expression was 13.3, 10.5, 13.4, 16.15, 18.1, and 25.05 in PTX, TQ, PTX + TQ 25 μ M, PTX + TQ 50 μ M, PTX + TQ 75 μ M, and PTX + TQ 100 μ M groups (***) P-value < 0.001, ns: non-significant). ATG-5 overexpressed in all experimental groups with nearly the most significant differences, where ATG-5 increment was 2.33, 2.17, 3.03, 4.57, 7.67, and 12.9 in PTX, TQ, PTX + TQ 25 μ M, PTX + TQ 50 μ M, PTX + TQ 75 μ M, and PTX + TQ 100 μ M groups (***) P-value < 0.001, ns: non-significant). ATG-7 overexpression was evident in all experimental groups with prominent differences. ATG-7 expression values were 3.5, 4.43,

6.45, 7.66, 15.82, and 19.41 in PTX, TQ, PTX + TQ 25 μ M, PTX + TQ 50 μ M, PTX + TQ 75 μ M, and PTX + TQ 100 μ M groups (***) P-value < 0.001).

Discussion

In the present experiment, we explored the impact of PTX and TQ combinations on inhibiting invasive BC by regulating intracellular death pathways. BC is a high-incidence cancer and the main reason for cancer-associated deaths among women throughout the world [15]. Multimodal strategies comprising surgery, chemotherapy, radiotherapy, and endocrine therapy have been developed to suppress various types of BC at early stages to advanced states. In metastatic BC, however, surgical interventions would be a palliatory option for the patient rather than a survival-beneficial point [16]. Over several decades, systemic cytotoxic chemotherapy has been the critical therapeutic option for invasive BC in the clinic, focusing on hormone receptor-positive (HR+), HER-2+, and triple-negative tumors [17]. However, no chemotherapeutic protocol is ultimately acceptable as the

first-line treatment for invasive BC [18]. PTX resistance occurs due to β -tubulin mutations and the upregulation of tubulin binding protein tau, ER, HER2, BRCA1, and multi-drug resistance protein (MDR1) [8].

The drug combination has a long history that returns to traditional Chinese medicine, where combining multiple herbal formulations was being applied for treating diseases relevant to the skin (atopic dermatitis), respiratory (bronchial asthma), and gastro-intestinal (irritable bowel syndrome) systems [19]. One of the first attempts to administer drug combination for BC was prolonged cyclic treatment with cyclophosphamide, methotrexate, and fluorouracil as adjuvant treatment in metastatic BC. Long-term chemotherapy yielded an appealing toxicity, allowing a high percentage of drug dosage administration. However, the influence of combination therapy on patients' long-term survival and possible adverse effects remains unclear [20].

Combining chemotherapeutics with natural phytochemicals has been attractive for developing improved strategies with enhanced efficacy and reduced systemic toxicities [21]. Our results showed that single PTX and TQ could inhibit MDA-MB-231 cell proliferation dose-dependently. Previous studies have documented that PTX hindered MCF-7 cell growth and invasiveness and triggered apoptosis by downregulating the PI3K/AKT signaling pathway [22]. TQ targeted cyclin D1/E and P27 by which, preventing cell division progression at the G1/S phase [23]. It also suppressed BC cell proliferation in a mouse xenograft model through ROS production, P38 phosphorylation, and the inhibition of pro-apoptotic proteins [24].

Our results revealed that combined treatments could yield antagonism effects at low PTX concentrations, which shifted into additive and synergistic effects at higher PTX concentrations, followed by reduced IC₅₀ values. This finding agreed with what Alkhatib et al. reported, where docetaxel (DTX) and TQ had antagonist effects against MCF-7 and MDA-MB-231 cells. They formulated DTX and TQ in borage oil-based nano-emulsion to increase drug interactions and cellular uptake [25].

Increasing PTX concentrations could provide positive interactions with TQ, leading to enhanced anticancer effects. MTT data indicated that drug combinations had a synergistic impact where adding TQ at 75 and 100 μ M concentrations reduced PTX IC₅₀ values to 9.6 and 16 folds, respectively. At the same time, the required dose of TQ for reaching 50% of cell proliferation was reduced to 2.5 folds. PTX induced apoptosis in cancer cells by Bcl-2 hyperphosphorylation and inactivation, depleting calcium ions from mitochondria and releasing cytochrome C [26, 27].

PTX alone or combined with carboplatin and gallic acid blocked cell cycle progress at the G2/M phase, leading to late-stage apoptotic death [28]. TQ significantly augmented

PTX potential in triggering apoptosis by overexpressing pro-apoptotic genes P53 and BAX and decreasing the expression of anti-apoptotic gene Bcl-2. TQ-mediated ROS production seems effective in P53 and BAX increment, Bcl-2 reduction, and apoptosis stimulation in MCF-7 cells [29]. Also, PTX/TQ combinations suppressed BC cells through the upregulation of tumor suppressors (P21, P53, Brca1, and Hic1) and apoptosis pathway components (Caspases 3, 7, and 12) [30, 31].

Autophagy is a highly conserved catabolic pathway and a cell survival mechanism ensuring cellular homeostasis by removing intracellular damaged components and recycling organelles and proteins [32]. Autophagy has a controversial role in cancer progression and suppression; on the one hand, it is vital for cancer cell transformation and supports cancer cell viability under hypoxic conditions at later stages of *in vivo* tumor formation [33, 34]. On the other hand, autophagy seems to have a tumor suppressor function in fully transformed cancer cells, as impaired autophagy is linked to malignant transformation and carcinogenesis, and autophagy induction in some cancer cells leads to cell death [34].

Our data showed that PTX, TQ, and their combinations induced autophagy in treated cells with high Beclin-1, ATG-5, and ATG-7 expression levels. Previous experiments reported paradoxical findings of the role of PTX and TQ in apoptosis/autophagy regulation. In one study, PTX induced autophagy in MDA-MB-231 cells by activating forkhead box transcription factor O1 (FOXO1). And that inhibiting autophagy stimulated apoptotic cell death in cells [35]. In another study, PTX-mediated apoptosis induction was associated with increased LC3-II/LC3-I ratio and autophagy stimulation in non-small cell lung cancer cells [36]. Besides, TQ inhibited Beclin-1 and LC3 in MDA-MB-231 cells, interrupting cancer cell proliferation, invasion, and angiogenesis [37]. However, the TQ and DXT combination enhanced the autophagic vesicle formation, followed by cell death in MDA-MB-231 and MCF-7 cell lines [25]. Furthermore, TQ prevented ACHN and 786-O renal cancer cells from migrating and invading by activating AMPK/mTOR signaling and inducing autophagy [38].

Conclusion

Our *in vitro* findings suggest that adding phytochemicals into chemotherapy regimens could reduce the effective drug doses and the possible systemic toxicities while enhancing anticancer effects and tumor suppressive functions. Nevertheless, the precise interaction of co-treatment compounds and antagonistic impact should be explored in future investigations, *in vitro* and *in vivo*.

Acknowledgements The authors acknowledge the Fertility and Infertility Research Center, Health Technology Institute, Kermanshah University of Medical Sciences, Kermanshah, Iran, for their equipment and facilities support.

Author contributions A.B designed the study. A.B., M.B., and A.M. performed the experiment, processed and collected data. A.B., and M.Kh. analyzed and interpreted data. A.B. and MR.Kh. wrote the manuscript draft. M.Kh. and MR.Kh. revised the manuscript.

Funding This work was financially supported by the Kermanshah University of Medical Sciences, Kermanshah, Iran [grant No. 4020374].

Data availability No datasets were generated or analysed during the current study.

Declarations

Ethical approval The ethics committee of the Kermanshah University of Medical Sciences approved that this work complied with their ethical guidelines [Ethical code: IR.KUMS.MED.REC.1402.091].

Competing interests The authors declare no competing interests.

References

- Sung H, Ferlay J, Siegel RL, Laversanne M, Soerjomataram I, Jemal A, Bray F (2021) Global cancer statistics 2020: GLOBOCAN estimates of incidence and mortality worldwide for 36 cancers in 185 countries. *Cancer J Clin* 71(3):209–249. <https://doi.org/10.3322/caac.21660>
- Arnold M, Morgan A, Rungay H, Mafra A, Singh D, Laversanne M, Vignat J, Gralow JR, Cardoso F, Siesling S (2022) Current and future burden of breast cancer: global statistics for 2020 and 2040. *Breast* 66:15–23. <https://doi.org/10.1016/j.breast.2022.08.010>
- Gupta GK, Collier AL, Lee D, Hoefler RA, Zheleva V, van Siewertsz LL, Tang-Tan AM, Guye ML, Chang DZ, Winston JS, Samli B, Jansen RJ, Petricoin EF, Goetz MP, Bear HD, Tang AH (2020) Perspectives on triple-negative breast Cancer: current treatment strategies, unmet needs, and potential targets for future therapies. *Cancers* 12(9):2392. <https://doi.org/10.3390/cancers12092392>
- Bozorgi A, Bozorgi M, Khazaei M (2022) Immunotherapy and immunoengineering for breast cancer; a comprehensive insight into CAR-T cell therapy advancements, challenges and prospects. *Cell Oncol* 45(5):755–777. <https://doi.org/10.1007/s13402-022-00700-w>
- Abu Samaan TM, Samec M, Liskova A, Kubatka P, Büsselfeld D (2019) Paclitaxel's mechanistic and clinical effects on breast Cancer. *Biomolecules* 9(12):789. <https://doi.org/10.3390/biom9120789>
- Zhu L, Chen L (2019) Progress in research on paclitaxel and tumor immunotherapy. *Cell Mol Biol Lett* 24(1):40. <https://doi.org/10.1186/s11658-019-0164-y>
- Bernabeu E, Cagel M, Lagomarsino E, Moretton M, Chiappetta DA (2017) Paclitaxel: what has been done and the challenges remain ahead. *Inte J Pharm* 526(1):474–495. <https://doi.org/10.1016/j.ijpharm.2017.05.016>
- Maloney SM, Hoover CA, Morejon-Lasso LV, Prospero JR (2020) Mechanisms of Taxane Resistance. *Cancers* 12(11):3323. <https://doi.org/10.3390/cancers12113323>
- Bayat Mokhtari R, Homayouni TS, Baluch N, Morgatskaya E, Kumar S, Das B, Yeager H (2017) Combination therapy in combating cancer. *Oncotarget* 8(23):38022–38043. <https://doi.org/10.18632/oncotarget.16723>
- Almajali B, Al-Jamal HAN, Taib WRW, Ismail I, Johan MF, Doolanea AA, Ibrahim WN (2021) Thymoquinone, as a Novel Therapeutic candidate of cancers. *Pharmaceuticals* 14(4):369. <https://doi.org/10.3390/ph14040369>
- Bozorgi A, Khazaei S, Khademi A, Khazaei M (2020) Natural and herbal compounds targeting breast cancer, a review based on cancer stem cells. *Iran J Basic Med Sci* 23(8):970–983. <https://doi.org/10.22038/ijbms.2020.43745.10270>
- Saghatelian T, Tananyan A, Janoyan N, Tadevosyan A, Petrosyan H, Hovhannisyan A, Hayrapetyan L, Arustamyan M, Arnhold J, Rotmann A-R (2020) Efficacy and safety of curcumin in combination with paclitaxel in patients with advanced, metastatic breast cancer: a comparative, randomized, double-blind, placebo-controlled clinical trial. *Phytomedicine* 70:153218. <https://doi.org/10.1016/j.phymed.2020.153218>
- Chou J, Chou T (1991) Quantitation of synergism and antagonism of two or more drugs by computerized analysis. *Synergism Antagonism Chemother*: 223–244
- Iannelli F, Roca MS, Lombardi R, Ciardiello C, Grumetti L, De Rienzo S, Moccia T, Vitagliano C, Sorice A, Costantini S, Milone MR, Pucci B, Leone A, Di Gennaro E, Mancini R, Ciliberto G, Bruzzese F, Budillon A (2020) Synergistic antitumor interaction of valproic acid and simvastatin sensitizes prostate cancer to docetaxel by targeting CSCs compartment via YAP inhibition. *J Exp Clin Cancer Res* 39(1):213. <https://doi.org/10.1186/s13046-020-01723-7>
- Harbeck N, Gnant M (2017) Breast cancer. *Lancet* 389(10074):1134–1150. [https://doi.org/10.1016/s0140-6736\(16\)31891-8](https://doi.org/10.1016/s0140-6736(16)31891-8)
- Vogel CL, Cobleigh MA, Tripathy D, Gutheil JC, Harris LN, Fehrenbacher L, Slamon DJ, Murphy M, Novotny WF, Burchmore M, Shak S, Stewart SJ, Press M (2023) Efficacy and Safety of Trastuzumab as a single Agent in First-Line treatment of HER2-Overexpressing metastatic breast Cancer. *J Clin Oncol* 41(9):1638–1645. <https://doi.org/10.1200/jco.22.02516>
- Koh SJ, Ohsumi S, Takahashi M, Fukuma E, Jung KH, Ishida T, Dai MS, Chang CH, Dalvi T, Walker G, Bennett J, O'Shaughnessy J, Balmaña J (2022) Correction to: prevalence of mutations in BRCA and homologous recombination repair genes and real-world standard of care of Asian patients with HER2-negative metastatic breast cancer starting first-line systemic cytotoxic chemotherapy: subgroup analysis of the global BREAKOUT study. *Breast Cancer* 29(1):189–190. <https://doi.org/10.1007/s12282-021-01299-w>
- Petrovic N, Sami A, Martinovic J, Zaric M, Nakashidze I, Lukic S, Jovanovic-Cupic S (2017) TIMP-3 mRNA expression levels positively correlates with levels of miR-21 in situ BC and negatively in PR positive invasive BC. *Pathol Res Pract* 213(10):1264–1270. <https://doi.org/10.1016/j.prp.2017.08.012>
- Drucker AM, Morra DE, Prieto-Merino D, Ellis AG, Yiu ZZN, Rochweg B, Di Giorgio S, Arents BW, Burton T, Spuls PI, Schmitt J, Flohr C (2022) Systemic immunomodulatory treatments for atopic dermatitis: update of a Living Systematic Review and Network Meta-Analysis. *JAMA Dermatol* 158(5):523–532. <https://doi.org/10.1001/jamadermatol.2022.0455>
- Saltz LB, Clarke S, Diaz-Rubio E, Scheithauer W, Figer A, Wong R, Koski S, Lichinitser M, Yang TS, Rivera F, Couture F, Sirzén F, Cassidy J (2023) Bevacizumab in Combination with oxaliplatin-based chemotherapy as first-line therapy in metastatic colorectal Cancer: a Randomized Phase III Study. *J Clin Oncol* 41(21):3663–3669. <https://doi.org/10.1200/jco.22.02760>
- Ferraro MG, Piccolo M, Misso G, Santamaria R, Irace C (2022) Bioactivity and Development of Small Non-platinum

- Metal-based chemotherapeutics. *Pharmaceutics* 14(5):954. <https://doi.org/10.3390/pharmaceutics14050954>
22. Li G, Xu D, Sun J, Zhao S, Zheng D (2020) Paclitaxel inhibits proliferation and invasion and promotes apoptosis of breast cancer cells by blocking activation of the PI3K/AKT signaling pathway. *Adv Clin Exp Med* 29(11):1337–1345. <https://doi.org/10.17219/acem/127681>
 23. Talib WH (2017) Regressions of breast carcinoma syngraft following treatment with piperine in combination with thymoquinone. *Sci Pharm* 85(3):27. <https://doi.org/10.3390/scipharm85030027>
 24. Woo CC, Hsu A, Kumar AP, Sethi G, Tan KHB (2013) Thymoquinone inhibits tumor growth and induces apoptosis in a breast cancer xenograft mouse model: the role of p38 MAPK and ROS. *PLoS ONE* 8(10):e75356. <https://doi.org/10.1371/journal.pone.0075356>
 25. Alkhatib MH, Bawadud RS, Gashlan HM (2020) Incorporation of docetaxel and thymoquinone in borage nanoemulsion potentiates their antineoplastic activity in breast cancer cells. *Sci Rep* 10(1):18124. <https://doi.org/10.1038/s41598-020-75017-5>
 26. Zhao S, Tang Y, Wang R, Najafi M (2022) Mechanisms of cancer cell death induction by paclitaxel: an updated review. *Apoptosis* 27(9):647–667. <https://doi.org/10.1007/s10495-022-01750-z>
 27. Khing TM, Choi WS, Kim DM, Po WW, Thein W, Shin CY, Sohn UD (2021) The effect of paclitaxel on apoptosis, autophagy and mitotic catastrophe in AGS cells. *Sci Rep* 11(1):23490. <https://doi.org/10.1038/s41598-021-02503-9>
 28. Aborehab NM, Elnagar MR, Waly NE (2021) Gallic acid potentiates the apoptotic effect of paclitaxel and carboplatin via over-expression of Bax and P53 on the MCF-7 human breast cancer cell line. *J Biochem Mol Toxicol* 35(2):e22638. <https://doi.org/10.1002/jbt.22638>
 29. Bhattacharjee M, Upadhyay P, Sarker S, Basu A, Das S, Ghosh A, Ghosh S, Adhikary A (2020) Combinatorial therapy of Thymoquinone and Emodin synergistically enhances apoptosis, attenuates cell migration and reduces stemness efficiently in breast cancer. *Biochim Biophys Acta Gen Subj* 1864(11):129695. <https://doi.org/10.1016/j.bbagen.2020.129695>
 30. Soni P, Kaur J, Tikoo K (2015) Dual drug-loaded paclitaxel–thymoquinone nanoparticles for effective breast cancer therapy. *J Nanoparticle Res* 17(1):18. <https://doi.org/10.1007/s11051-014-2821-4>
 31. Şakalar Ç, İzgi K, İskender B, Sezen S, Aksu H, Çakır M, Kurt B, Turan A, Canatan H (2016) The combination of thymoquinone and paclitaxel shows anti-tumor activity through the interplay with apoptosis network in triple-negative breast cancer. *Tumor Biol* 37(4):4467–4477. <https://doi.org/10.1007/s13277-015-4307-0>
 32. Li W, He P, Huang Y, Li Y-F, Lu J, Li M, Kurihara H, Luo Z, Meng T, Onishi M (2021) Selective autophagy of intracellular organelles: recent research advances. *Theranostics* 11(1):222–256. <https://doi.org/10.7150/thno.49860>
 33. Boyer-Guittaut M, Poillet L, Liang Q, Bôle-Richard E, Ouyang X, Benavides GA, Chakrama F-Z, Fraichard A, Darley-Usmar VM, Despouy G (2014) The role of GABARAP1/GEC1 in autophagic flux and mitochondrial quality control in MDA-MB-436 breast cancer cells. *Autophagy* 10(6):986–1003. <https://doi.org/10.4161/auto.28390>
 34. Patergnani S, Missiroli S, Morciano G, Perrone M, Mantovani CM, Anania G, Fiorica F, Pinton P, Giorgi C (2021) Understanding the role of Autophagy in Cancer formation and progression is a real opportunity to treat and cure human cancers. *Cancers* 13(22). <https://doi.org/10.3390/cancers13225622>
 35. Xu K, Zhu W, Xu A, Xiong Z, Zou D, Zhao H, Jiao D, Qing Y, Jamal MA, Wei HJ, Zhao HY (2022) Inhibition of FOXO1–mediated autophagy promotes paclitaxel–induced apoptosis of MDA-MB–231 cells. *Mol Med Rep* 25(2). <https://doi.org/10.3892/mmr.2022.12588>
 36. Park J-H, Park S-A, Lee Y-J, Park H-W, Oh S-M (2020) PBK attenuates paclitaxel-induced autophagic cell death by suppressing p53 in H460 non-small-cell lung cancer cells. *FEBS Open Bio* 10(5):937–950. <https://doi.org/10.1002/2211-5463.12855>
 37. Ünal TD, Hamurcu Z, Delibaşı N, Çınar V, Güler A, Gökçe S, Nurdinov N, Ozpolat B (2021) Thymoquinone inhibits proliferation and migration of MDA-MB-231 triple negative breast cancer cells by suppressing autophagy, Beclin-1 and LC3. *Anticancer Agents Med Chem*. 2021;21(3):355–364. <https://doi.org/10.2174/1871520620666200807221047>
 38. Zhang Y, Fan Y, Huang S, Wang G, Han R, Lei F, Luo A, Jing X, Zhao L, Gu S (2018) Thymoquinone inhibits the metastasis of renal cell cancer cells by inducing autophagy via AMPK/mTOR signaling pathway. *Cancer Sci* 109(12):3865–3873. <https://doi.org/10.1111/cas.13808>

Publisher's Note Springer Nature remains neutral with regard to jurisdictional claims in published maps and institutional affiliations.

Springer Nature or its licensor (e.g. a society or other partner) holds exclusive rights to this article under a publishing agreement with the author(s) or other rightsholder(s); author self-archiving of the accepted manuscript version of this article is solely governed by the terms of such publishing agreement and applicable law.